

Supplementary Information

Anomalous Phase Transition Behavior in Hydrothermal Grown Layered Tellurene

Han Li¹, Kedi Wu¹, Sijie Yang¹, Tara Boland¹, Bin Chen¹, Arunima K. Singh², and Sefaattin Tongay^{1,*}

¹ School for Engineering of Matter, Transport and Energy, Arizona State University, Tempe, Arizona 85287, USA

² Department of Physics, Arizona State University, Tempe, AZ 85287, USA

* corresponding authors: sefaattin.tongay@asu.edu

Density Functional Theory Simulations: In order to understand the abnormal Raman peak pressure dependence after 6.9 GPa during compression as well as between 3.4 and 6.9 GPa during decompression, we used density-functional theory simulations (DFT) to compute the pressure dependent structures, energies and Raman active modes of six Te phases from 0 to 9 GPa. The candidate structures were taken from the Materials Project (MP)¹ database. Note that only the crystal structures which have a corresponding ICSD² id (i.e. they have been experimentally synthesized) and are not duplicates were imported from the MP database. Based on these constraints we find six tellurium phases as possible candidates (structures shown in Table. S1), namely the trigonal phase, with MP material-id mp-19, three orthorhombic phases, with material-ids mp-105, mp-1064307 and mp-9924, the monoclinic phase, mp-570459, and the cubic phase, mp-10654.

A k -point mesh of $10 \times 10 \times 10$ with a 600 eV energy cutoff results in an accuracy of the total energies of 5 meV/unit cell. The structures are relaxed until the forces on the atoms are less than 0.005 eV/Å. The calculations of the normal mode phonon frequencies (including the Raman active as well as IR active modes) at the Γ point were performed using density-functional perturbation theory (DFPT) simulations on the primitive unit cell of the materials at the various pressures. Irreducible representation of normal modes are obtained from the PHONOPY program³ and the Bilbao Crystallographic Server⁴.

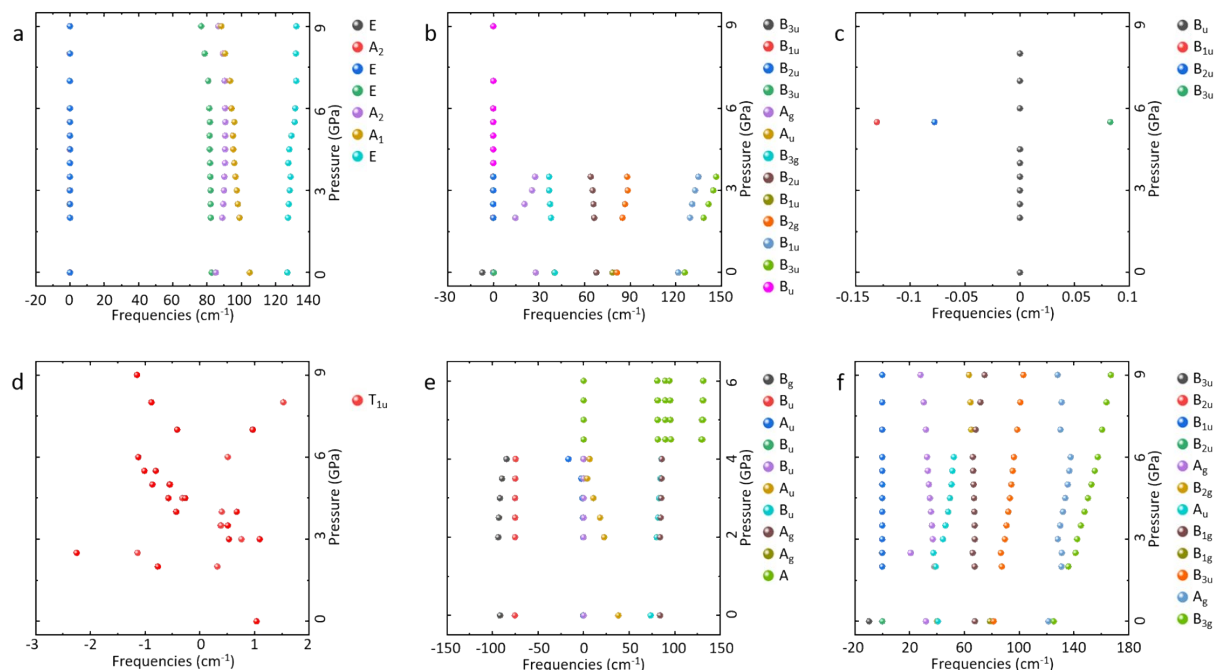


Figure S1. Simulated normal mode frequencies of **a.** the trigonal mp-19 **b.** the orthorhombic mp-105 **c.** the orthorhombic mp-9924 **d.** the cubic mp-10654 **e.** the monoclinic mp-570459 **f.** the orthorhombic mp-1064307 phases of tellurium between 0 and 9 GPa.

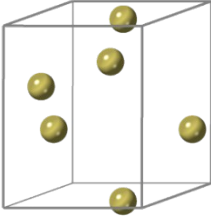
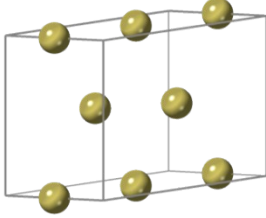
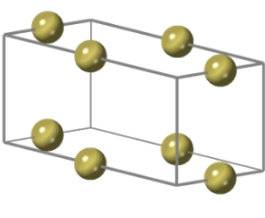
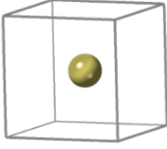
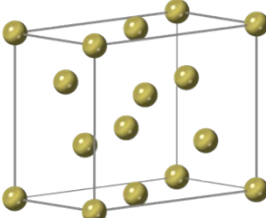
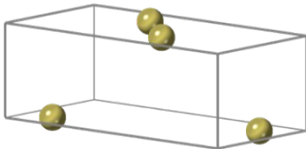
a		b		c	
mp-19 trigonal		mp-105 orthorhombic		mp-9924 orthorhombic	
d		e		f	
mp-10654 cubic		mp-570459 monoclinic		mp-1064307 orthorhombic	

Table S1. Unit cell structure of **a.** the trigonal mp-19 **b.** the orthorhombic mp-105 **c.** the orthorhombic mp-9924 **d.** the cubic mp-10654 **e.** the monoclinic mp-570459 **f.** the orthorhombic mp-1064307 phases of tellurium at zero pressure.

Phase	a (Å)	b (Å)	c (Å)	α (°)	β (°)	γ (°)	Space Group
mp-19	4.48	4.48	5.99	90	90	120	$P3_121$
mp-105	9.19	3.18	4.52	90	90	90	$Pmma$
mp-9924	3.08	7.41	3.00	90	90	90	$Cmmm$
mp-10654	3.21	3.21	3.21	90	90	90	$Pm\bar{3}m$
mp-570459	7.66	4.35	5.97	90	90.7	90	$C2/m$
mp-1064307	4.52	9.20	3.18	90	90	90	$Pbcm$

Table S2. DFT simulated lattice parameters and space groups of the six tellurium phases at zero pressure.

References

1. A. Jain; S. P. Ong; G. Hautier; W. Chen; W. D. Richards; S. Dacek; S. Cholia; D. Gunter; D. Skinner; G. Ceder; K. A. Persson. *APL Materials* **2013**, 1, (1), 011002.
2. A. Belsky; M. Hellenbrandt; V. L. Karen; P. Luksch. *Acta Crystallographica Section B* **2002**, 58, (3 Part 1), 364-369.
3. A. Togo; I. Tanaka. *Scripta Materialia* **2015**, 108, 1-5.
4. M. I. Aroyo; A. Kirov; C. Capillas; J. M. Perez-Mato; H. Wondratschek. *Acta Crystallographica Section A* **2006**, 62, (2), 115-128.